Two Distinct Motifs within the p53 Transactivation Domain Bind to the Taz2 Domain of p300 and Are Differentially Affected by Phosphorylation†

Lisa M. Miller Jenkins,‡,§ Hiroshi Yamaguchi,‡,§,|| Ryo Hayashi,§ Scott Cherry,⊥ Joseph E. Tropea,⊥ Maria Miller,⊥ Alexander Wlodawer,⊥ Ettore Appella,§ and Sharlyn J. Mazur*,§

Laboratory of Cell Biology, National Cancer Institute, National Institutes of Health, Bethesda, Maryland 20892, and Macromolecular Crystallography Laboratory, National Cancer Institute at Frederick, Frederick, Maryland 21702

Received September 9, 2008; Revised Manuscript Received December 5, 2008

ABSTRACT: The tumor suppressor p53 functions as a transcriptional activator for many genes, including several key genes involved in cell cycle arrest and apoptosis. Following DNA damage-induced stress, p53 undergoes extensive posttranslational modification, resulting in increased stability and activity. Two critical cofactors for p53-mediated transactivation are the histone acetyltransferase paralogues CREB-binding protein (CBP) and p300. The N-terminal transactivation domain of p53 interacts with several domains of CBP/p300, including the Taz2 domain. Here, we report the effects of specific p53 phosphorylations on its interaction with the Taz2 domain of p300. Using a competitive fluorescence anisotropy assay, we determined that monophosphorylation of p53 at Ser_{15} or Thr_{18} increased the affinity of p53(1−39) for Taz2, and diphosphorylations at Ser_{15} and Ser_{37} or Thr_{18} and Ser_{20} further increased the affinity. In addition, we identified a second binding site for Taz2 within p53 residues 35−59. This second site bound Taz2 with a similar affinity as the first site, but the binding was unaffected by phosphorylation. Thus, p53 posttranslational modification modulates only one of the two binding sites for p300 Taz2. Further investigation of Taz2 binding to p53(1−39) or p53(35−59) by isothermal titration calorimetry indicated that upon complex formation, the change in heat capacity at constant pressure, ΔC_p, was negative for both sites, suggesting the importance of hydrophobic interactions. However, the more negative value of ΔC_p for Taz2 binding to the first (−330 cal/(mol·K)) compared to the second site (−234 cal/(mol·K)) suggests that the importance of nonpolar and polar interactions differs between the two sites.

The tumor suppressor p53 regulates the transcription of many genes, including several key genes involved in apoptosis and cell cycle arrest (*1*). The p53 protein activates transcription, in part, through the recruitment of chromatin modifying factors, including the histone acetyltransferase paralogues CREB-binding protein (CBP)[1] and p300. It has been shown that p53-dependent recruitment of CBP/p300 to promoters facilitated local chromatin unwinding through histone modification (*2, 3*). Furthermore, upon DNA damage, p53 may be acetylated by CBP or p300 on six C-terminal lysine residues (*4, 5*).

CBP and p300 share a common domain structure. Near the N terminus is located the first of two transcriptional adaptor zinc-binding (Taz) domains, termed Taz1 or CH1 (*6*). The Taz1 domain has been shown to interact with a number of proteins, including HIF-1α and CITED2. Following the Taz1 domain is the KIX domain, first identified as the site of CREB interaction (*7*). In the central regions of CBP and p300 are the bromo- and acetyltransferase domains, both important for the enzymatic activity of the protein. The C-terminal regions contain the second Taz domain, Taz2, and the interferon binding domain (IBiD). Taz2 is a site of CBP/p300 interaction with E1A, GATA-1, and E2F, among others (*8*). The IBiD domain interacts with interferon regulatory factor 3, as well as Ets-2, E1A, and TIF-2 (*9*). An IBiD homology domain (IHD) has recently been described in p300 between the Taz1 and KIX domains (*10*).

Interaction of p53 with CBP/p300 has been shown to occur through several domains of CBP/p300: CH1/Taz1, IHD, KIX, CH3/Taz2, and IBiD (*10*−*16*). All of these domains interact with the N-terminal acidic transactivation domain (TAD) of p53. This domain of p53 can be further divided into two subdomains, TAD1 (residues 1−40) and TAD2 (residues 41−61) (*17, 18*). Both domains can function independently to activate transcription (*17*). Furthermore, distinct protein−protein interactions have been shown to

† This research was supported by the Intramural Research Program of the NIH, National Cancer Institute, Center for Center Research.

* Corresponding author. Phone: 301-435-6293. Fax: 301-435-8188. E-mail: mazurs@mail.nih.gov.

‡ L.M.M.J. and H.Y. contributed equally to this work.

§ Laboratory of Cell Biology, National Cancer Institute.

|| Current address: Nanotechnology Research Institute, National Institute of Advanced Industrial Science and Technology (AIST), 807-1 Shuku, Tosu, Saga 841-0052, Japan.

⊥ Macromolecular Crystallography Laboratory, National Cancer Institute at Frederick.

[1] Abbreviations: CBP, CREB-binding protein; CD, circular dichroism; DTT, dithiothreitol; EDTA, ethylenediaminetetraacetic acid; Fmoc, fluorenylmethoxycarbonyl; FRET, fluorescence resonance energy transfer; GST, glutathione *S*-transferase; IBiD, interferon binding domain; IHD, IBiD homology domain; IPTG, isopropyl β-D-thiogalactopyranoside; ITC, isothermal titration calorimetry; MBP, maltose binding protein; PBS, phosphate-buffered saline; PCR, polymerase chain reaction; RP-HPLC, reversed-phase high-performance liquid chromatography; SDS, sodium dodecyl sulfate; TAD, transactivation domain; Taz, transcriptional adaptor zinc binding; TEV, tobacco etch virus; TFA, trifluoroacetic acid.

10.1021/bi801716h CCC: $40.75
Published on Web 01/23/2009

occur for the two domains. For example, interactions between p53 and its negative regulators MDM2 and MDM4 occur primarily through TAD1 (*19*−*21*), while interactions with RPA and the p62 subunit of TFIIH occur through TAD2 (*22*−*25*).

Following DNA damage-induced stress, both TAD subdomains of p53 become extensively phosphorylated (*26*), activating p53 and increasing its stability by disrupting the binding of MDM2, thereby preventing p53 ubiquitylation and degradation (*19, 27*). Phosphorylation has also been shown to affect the interaction of p53 with other proteins. For example, phosphorylation of p53 at Thr_{18} weakens binding of MDM2 (*19, 27*), while phosphorylation of p53 at Ser_{46} and Thr_{55} increases its affinity for the p62 subunit of TFIIH (*23*). Furthermore, phosphorylation of p53 at Ser_{15} was shown *in vitro* to increase binding of CBP/p300 (*28, 29*). Thus, posttranslational modification of p53 modulates its protein−protein interactions and, thereby, regulates its activity and stability.

Recent studies have systematically examined the binding of the p53 TAD to several domains of CBP/p300. Teufel et al. examined the binding of the p53 TAD to the Taz1, KIX, Taz2, and IBiD domains of p300, finding that p53(1−57) binds to each of the four domains with moderate to high affinity (*30*). Polley et al. examined the effect of phosphorylation on the binding of p53(1−39) to the IBiD, IHD, and Taz1 domains of p300 (*31*). They showed that p53 phosphorylation was required for interaction with the IHD domain and strengthened interactions with the IBiD and CH1/Taz1 domains. Interestingly, diphosphorylation of p53(1−39) at Ser_{15} and Ser_{20} reduced binding to the IHD and CH1/Taz1 domains compared with the monophosphorylated forms but moderately increased the affinity for the IBiD domain (*31*).

To further understand the role of phosphorylation in the regulation of p53 interactions, we investigated the affinity of phosphorylated forms of the p53 TAD for the Taz2 domain of p300. Using fluorescence anisotropy, we have determined the effect of various mono-, di-, and triphosphorylations on binding of p53(1−39) to Taz2, some of which significantly increased binding. Furthermore, we observed that Taz2 bound to p53 TAD2 with an affinity comparable to that of the TAD1 site, but the affinity was not affected by phosphorylation. Isothermal titration calorimetry (ITC) experiments were used to compare the thermodynamics of Taz2 binding to TAD1 and TAD2 to better understand the differences in binding by the two sites. We can thus describe two binding sites on p53 for Taz2 and provide further evidence for the importance of p53 posttranslational modifications in the regulation of its protein−protein interactions.

EXPERIMENTAL PROCEDURES

Protein Expression and Purification. Two versions of the human p300 Taz2 domain, A_{1723}−Q_{1843} and A_{1723}−K_{1812}, were amplified from full-length cDNA (obtained from P. Johnson, NCI) using polymerase chain reaction (PCR) with the following oligonucleotide primers: 5′-GAG AAC CTG TAC TTC CAG GCT ACC CAG AGC CCA GGC GAT TC-3′ (forward primer) and 5′-GGG GAC CAC TTT GTA CAA GAA AGC TGG GTT ATT ACT GCC CAA CCA CAC CAG TCC GCT G-3′ (reverse primer 1) for A_{1723}−Q_{1843}, and forward primer and 5′-GGG GAC CAC TTT GTA CAA GAA AGC TGG GTT ATT ACT TCT GCT TGA TGT TTA GGC AGA AC-3′ (reverse primer 2) for A_{1723}−K_{1812}. The PCR amplicons were subsequently used as templates for a second round of PCR with the following primers: 5′-GGG GAC AAG TTT GTA CAA AAA AGC AGG CTC GGA GAA CCT GTA CTT CCA G-3′ and reverse primer 1 or 2 for A_{1723}−Q_{1843} or A_{1723}−K_{1812}, respectively. The amplicons from the second PCR were inserted by recombinational cloning into the vector pDONR201 (Invitrogen, Carlsbad, CA), and the nucleotide sequences of the entry clones were confirmed by DNA sequencing. Four cysteine-to-alanine mutations, at positions 1738, 1746, 1789, and 1790, were introduced into the entry clone containing the Taz2 domain for A_{1723}−K_{1812} using the QuikChange mutagenesis kit (Stratagene, La Jolla, CA). The open reading frame encoding either of the Taz2 domains of p300, combined with a recognition site for tobacco etch virus (TEV) protease on the N terminus (ENLYFQ/A), was moved by recombinational cloning into the destination vector pKM596 to produce pJT16 or pJT57. pJT16 and pJT57 direct the expression of the wt Taz2 (A_{1723}−Q_{1843}) and 4CA-Taz2 (A_{1723}−K_{1812}/C1738A, C1746A, C1789A, C1790A), respectively, as a fusion protein with *Escherichia coli* maltose binding protein (MBP) with an intervening TEV protease recognition site. The fusion proteins were expressed in the *E. coli* strain BL21-CodonPlus (DE3)-RIL (Stratagene, La Jolla, CA). Cells were grown to midlog phase ($OD_{600} \sim 0.5$) at 37 °C in Luria broth containing 100 μg/mL ampicillin, 35 μg/mL chloramphenicol, 100 μM $ZnCl_2$, and 0.2% glucose. Overproduction of fusion protein was induced with isopropyl β-D-thiogalactopyranoside (IPTG) at a final concentration of 1 mM for 4 h at 30 °C. The cells were pelleted by centrifugation and stored at −80 °C.

Cell paste was suspended in ice-cold 50 mM Tris·HCl (pH 7.5) and 500 mM NaCl (buffer A) containing 1 mM ethylenediaminetetraacetic acid (EDTA), 1 mM 1,4-dithio-DL-threitol (DTT), and Complete protease inhibitor cocktail (Roche Diagnostics, Mannheim, Germany). Cells were disrupted with an APV-1000 homogenizer (Invensys, Roholmsvej, Denmark) at 10000 psi, and centrifuged at 30000*g* for 30 min. The supernatant was filtered through a 0.45 μm cellulose acetate membrane and applied to an amylose column (New England Biolabs, Beverly, MA) equilibrated in buffer A. The column was washed and eluted with 30 mM maltose in buffer A. Fractions containing recombinant fusion protein were digested with MBP-TEV protease overnight at 4 °C. The digest was applied to a Zn^{2+}-agarose column equilibrated in buffer A, washed, and eluted with 500 mM imidazole in buffer A. Fractions containing the Taz2 domain were pooled and incubated overnight at 4 °C in the presence of 10 mM DTT and 10 mM $ZnCl_2$. The pool was concentrated using a YM3 membrane (Millipore Corp., Bedford, MA) and applied to a HiLoad 26/60 Superdex 75 prep grade column equilibrated in 20 mM Tris·HCl (pH 7.5) and 500 mM NaCl. Fractions containing the recombinant Taz2 domain were pooled and concentrated as above. The final products were judged to be >95% pure on the basis of silver staining after sodium dodecyl sulfate (SDS)−polyacrylamide gel electrophoresis. Protein concentrations were estimated spectrophotometrically using a molar extinction coefficient of 1490 M^{-1} cm^{-1} (280 nm) for both Taz2 domains. The molecular weights of the recombinant

proteins were confirmed using electrospray ionization mass spectrometry.

The coding sequence for human MDM2(17−125) was PCR amplified from a plasmid containing MDM2(1−125) with the following oligonucleotide primers: 5′-AAA GGA TCC CAG ATT CCA GCT TCG GAA CAA-3′ and 5′-CCC GAA TTC CTA GTT CTC ACT CAC AGA TGT-3′ (*32*). The amplified coding sequence was subcloned into pGEX4T-1 (GE Healthcare, Piscataway, NJ) using the *Bam*HI and *Eco*RI restriction sites and expressed in *E. coli* BL21(DE3) as a glutathione *S*-transferase (GST) fusion protein. Protein expression was induced with 1 mM IPTG at 30 °C for 4 h. The cells were resuspended in 50 mM Tris·HCl (pH 8), 120 mM NaCl, 0.5% NP-40, and 2 mM DTT (EBC buffer) and protease inhibitors (Roche Applied Science, Indianapolis, IN), lysed by French press, and centrifuged at 13000*g* for 1 h. The supernatant was incubated for 1 h at 4 °C with glutathione−Sepharose (GE Healthcare, Piscataway, NJ) equilibrated with EBC buffer. The bound fusion protein was then equilibrated in phosphate-buffered saline (PBS) and digested with 100 units of thrombin (EMD Biosciences, Gibbstown, NJ) for 4 h at 25 °C to remove the MDM2(17−125) from the GST. The cleaved MDM2(17−125) was found to be >90% pure by SDS gel electrophoresis.

Peptide Synthesis and Purification. Peptides were synthesized by the solid-phase method with 9-fluorenylmethoxycarbonyl (Fmoc) chemistry. Phosphoamino acids were coupled as Fmoc-Thr[PO(OBzl)OH]-OH and Fmoc-Ser-[PO(OBzl)OH]-OH (Novabiochem, San Diego, CA). Fluorescence labeling of the peptide was achieved with 3 equiv of 5(6)-carboxyfluorescein succiniimidyl ester (Molecular Probes, Eugene, OR) in dimethyl sulfoxide stirred overnight at 25 °C in the dark. The peptides were cleaved with a solution of 82.5% trifluoroacetic acid (TFA), 5% phenol, 5% thioanisole, 5% water, and 2.5% ethanedithiol and then purified by reversed-phase high-performance liquid chromatography (RP-HPLC) on a C-4 column with 0.05% TFA/water/acetonitrile. The purity of the peptides was determined to be >95% by analytical RP-HPLC. The mass of peptides was confirmed by matrix-assisted laser desorption ionization time-of-flight mass spectrometry (Micromass, Beverly, MA). The extinction coefficients for p53(1−39) and p53(35−59) were calculated from the amino acid composition (*33*). The extinction coefficient for p53(1−57) was determined by quantitative amino acid composition analysis of the purified peptide. Based upon the concentrations of five amino acids (Phe, Thr, Val, Lys, Ala) for which the measured concentration fell between the 62 and 125 pmol standards, the extinction coefficient was calculated to be 6900 ± 200 M^{-1} cm^{-1}.

Fluorescence Polarization Binding Assay. The p300 Taz2 domain (wt Taz2 or 4CA-Taz2) or MDM2(17−125) protein (0.001−100 μM) was incubated with 10 nM fluorescein-labeled human p53(14−28), fluorescein-LSQETFSDL-WKLLPE, in 20 mM acetate buffer (pH 6.0), 200 mM NaCl, 5% glycerol, 3.0 equiv of $ZnCl_2$, and 0.1 mg/mL BSA overnight at 4 °C. Fluorescence anisotropy was measured at 25 °C on a Beacon 2000 (PanVera, Madison, WI). The equilibrium association constant K_s, was estimated by nonlinear curve fitting of the observed anisotropies to eq 1 (see, e.g., eqs 6 and 40 in ref *34*).

$$A_{obs} = A_f + (A_b - A_f) \times \frac{K_s^{-1} + L_{ST} + R_T - \sqrt{(K_s^{-1} + L_{ST} + R_T)^2 - 4L_{ST}R_T}}{2L_{ST}} \quad (1)$$

A_{obs}, A_f, and A_b indicate the observed, free, and bound anisotropies and L_{ST} and R_T are the total concentrations of the labeled peptide and protein, respectively. Nonlinear curve fitting was done using Origin software (MicroCal, Northhampton, MA).

Equilibrium association constants for the binding of nonlabeled p53 peptides to p300 Taz2 domains were determined by a fluorescence anisotropy competition assay. Samples of p53 peptides (0.001−300 μM), 1.0 μM wt Taz2 or 4CA-Taz2, and 10 nM fluorescein-labeled p53(14−28) peptide were incubated overnight at 4 °C in 10 mM acetate buffer (pH 6.0), 200 mM NaCl, 5% glycerol, 6 μM $ZnCl_2$, and 0.1 mg/mL BSA. Fluorescence anisotropies were measured at 25 °C. The equilibrium association constants, K_a, were estimated by nonlinear curve fitting of the observed anisotropies to the solution of the cubic competitive binding equation (*34*):

$$A_{obs} = A_f + (A_b - A_f)\left(\frac{2\sqrt{(f^2 - 3g)}\cos(\theta/3) - f}{(3/K_s) + 2\sqrt{(f^2 - 3g)}\cos(\theta/3) - f}\right) \quad (2)$$

where

$$f = K_s^{-1} + K_a^{-1} + L_{ST} + L_T - R_T$$

$$g = \frac{L_T - R_T}{K_s} + \frac{L_{ST} - R_T}{K_a} + \frac{1}{K_s K_a}$$

$$\theta = \arccos\left(\frac{-2f^3 + 9fg + 27R_T/K_s K_a}{2\sqrt{(f^2 - 3g)^3}}\right)$$

L_T denotes the total concentration of the nonlabeled peptide.

Circular Dichroism (CD) Measurement. Either wt Taz2 or 4CA-Taz2 (15 μM) was dissolved in 10 mM Tris·HCl (pH 8.0) with or without 250 μM EDTA and 300 μM DTT. Far-UV CD spectra were measured from 190 to 260 nm on a JASCO J-715 spectropolarimeter (Jasco, Inc., Easton, MD) using a quartz cuvette with a path length of 1 mm at 25 °C. The spectra shown are plots of mean residue ellipticity averaged over eight scans and were corrected for background interference from the buffer.

Fluorescence Resonance Energy Transfer (FRET) Assay. 4CA-Taz2 and MDM2(17−125) were dialyzed into PBS before being labeled with DyLight 488 NHS ester (4CA-Taz2) or DyLight 549 NHS ester (MDM2(17−125) and 4CA-Taz2) (Pierce, Rockford, IL). Labeling was performed according to manufacturer's specifications at pH 7.2 to promote reaction specifically at the N terminus of the proteins. The labeled proteins were separated from the unincorporated dye using Bio-Gel P6 chromatography columns (Bio-Rad, Hercules, CA) according to manufacturer's instructions. Incorporation of the fluorescent labels was found to be 0.4 mol of DyLight 488/mol of 4CA-Taz2, 0.4 mol of DyLight 549/mol of MDM2(17−125), and 1.0 mol of DyLight 549/mol of 4CA-Taz2. FRET measurements were

performed using a SpectraMAX Gemini (Molecular Devices, Sunnyvale, CA) at 37 °C with excitation at 490 nm and emission detected at 580 nm. Competition assays were performed by incubating 0.75 μM 549-labeled 4CA-Taz2 with equimolar fluorescein-labeled p53(1−39) peptides with and without 0.75 μM MDM2(17−125) in 20 mM Tris·HCl (pH 7.4) and 100 mM NaCl for 1 h at 25 °C prior to reading. Assays to detect ternary complexes were performed by incubating 0.75 μM 488-labeled 4CA-Taz2 with either 0.75 μM 549-labeled MDM2(17−125) or 4CA-Taz2 in the presence of equimolar p53(1−57) in 20 mM Tris·HCl (pH 7.4) and 100 mM NaCl for 1 h at 25 °C prior to reading. Each of these experiments was performed at least twice.

Isothermal Titration Calorimetry (ITC). ITC measurements were performed using a VP-ITC calorimeter (MicroCal, Northhampton, MA). Titrations were performed in 20 mM Tris·HCl (pH 7.5), 100 mM NaCl, and 2 mM β-mercaptoethanol at 15, 25, or 35 °C as specified in the figure legends. Some experiments were performed in ITC buffer with 200 mM NaCl rather than 100 mM NaCl as specified. The concentrations of the injected peptides and proteins were determined from the absorbance at 280 nm. The protein and peptide solutions were degassed before each experiment. Heats of dilution were subtracted from the raw data. ITC experiments with p53(1−39) or p53(35−59) binding to 4CA-Taz2 were fit with a 1:1 binding model using ORIGIN software with the ITC package (Microcal, Northhampton, MA). All experiments were performed at least two times. ITC experiments with p53(1−57) binding to 4CA-Taz2 were fit to a model in which two Taz2 molecules bind to two nonidentical sites in p53(1−57). Binding of a single ligand (Taz2) to the first or second site on p53(1−57) is characterized by the association constant K_1 or K_2, respectively, and formation of the ternary complex is characterized by $K_3 = \alpha K_1 K_2$. Negative cooperativity in the binding of two Taz2 molecules is indicated when $\alpha < 1$. The concentrations of the three distinct p53-Taz2 complexes may be calculated from the total concentrations of p53(1−57) (M_T) and Taz2 (X_T) and expressions for the equilibrium constants and conservation of mass following the solution of a cubic equation in the free ligand concentration, X_f:

$$X_f = \frac{2}{3}\sqrt{a^2 - 3b}\cos(\theta/3) - \frac{a}{2} \quad (3)$$

where

$$a = (K_1 + K_2)/K_3 + 2M_T - X_T$$

$$b = (1 + (K_1 + K_2)(M_T - X_T))/K_3$$

$$\theta = \arccos\left(\frac{9ab + (27X_T/K_3) - 2a^3}{2\sqrt{(a^2 - 3b)^3}}\right)$$

The heat content of the solution at any point in the titration is given by

$$Q = M_T V_0 (f_1 \Delta H_1 + f_2 \Delta H_2 + f_3 \Delta H_3) \quad (4)$$

where f_1 and f_2 are the fractions of p53(1−57) with Taz2 bound to the first site or second site, respectively, ΔH_1 and ΔH_2 are the corresponding enthalpies of complex formation, and V_0 is the volume of the cell. The fraction of p53(1−57) with two Taz2 molecules bound is given by f_3, and the corresponding enthalpy of complex formation is $\Delta H_3 = \Delta H_1 + \Delta H_2 + \Delta H_\alpha$, where ΔH_α is the enthalpy of cooperativity. Displaced volume-corrected heats of injection were calculated according to standard ITC equations (Microcal, Northhampton, MA). This model was used to fit data from four ITC experiments, two with p53(1−57) in the syringe and two with p53(1−57) in the cell.

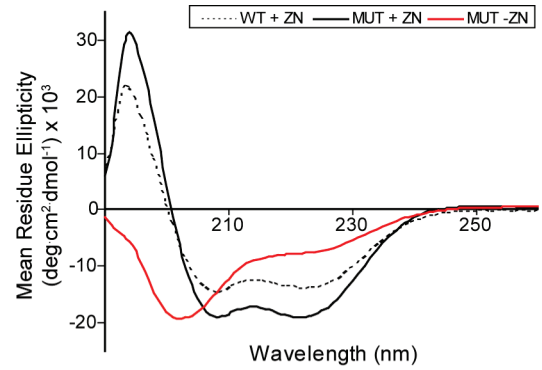

FIGURE 1: CD spectra of native wt Taz2 (black, dashed line) and 4CA-Taz2 (black, solid line). Also shown is the CD spectrum of 4CA-Taz2 in which the Zn^{2+} was removed (red, solid line) by incubation with a 100-fold molar excess of EDTA and a 20-fold molar excess of DTT for 1 h, 25 °C.

RESULTS

Characterization of Two Recombinant Human p300 Taz2 Domain Proteins. In the present work, we investigated the binding of p53 peptides to two versions of the human p300 Taz2 domain. The longer protein consists of the wild-type p300 sequence corresponding to residues 1723−1843 and will be referred to as wt Taz2. Based upon the alignment of the p300 and CBP Taz2 sequences, 9 of the 13 cysteines, along with 3 histidines, form 3 zinc-coordinating domains (*35*). In the shorter Taz2 protein, which corresponds to p300(1723−1812), the remaining four cysteine residues, Cys_{1738}, Cys_{1746}, Cys_{1789}, and Cys_{1790}, were mutated to alanine to yield a more stable protein; this protein will be referred to as 4CA-Taz2. In an earlier report on the structure of the highly similar Taz2 domain of CBP, the analogous mutant, in which the 4 non-zinc coordinating cysteines had been mutated to alanine, behaved like wild-type Taz2 in the presence of Zn^{2+} (*35*). As expected, we found that, in the presence of Zn^{2+}, the CD spectrum of 4CA-Taz2 was nearly identical to that of wt Taz2 and indicated the formation of α-helical structures in both preparations (Figure 1). Further, these CD spectra are similar to those previously reported for the Taz2 domain of CBP (*35*).

The Region of p53 That Interacts with the p300 Taz2 Domain Is More Extensive Than the Region That Interacts with MDM2. We first measured the binding to wt Taz2 of p53(14−28), the minimum domain for binding to MDM2-(17−125). The direct binding of fluorescein-labeled p53-(14−28) to wt Taz2 ($K_s = 4.5 \times 10^5$ M^{-1}) was significantly weaker than its binding to MDM2(17−125) ($K_s = 2.6 \times 10^6$ M^{-1}) (Figure 2A). The latter value is consistent with the reported value for the binding of p53 to MDM2 ($K_a = 1.7 \times 10^6$ M^{-1}) (*21*). The observed, relatively weak interaction between wt Taz2 and p53(14−28) is consistent with the previously reported weak binding of p53(14−28) to the Taz2 domain from CBP (*35*). Since the presence of the fluorescein label may affect the binding of peptides, we

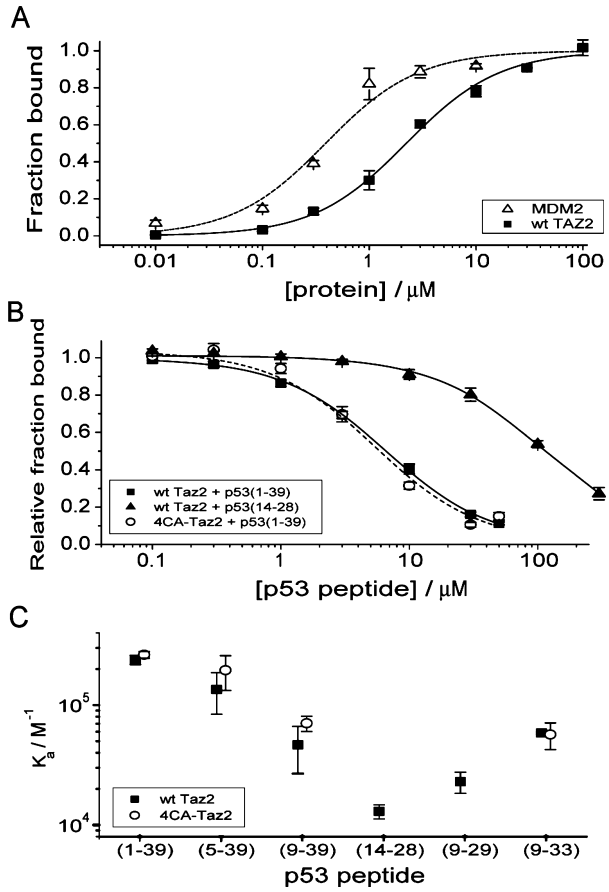

FIGURE 2: Length dependence of the interaction of p53 TAD1 peptides with wt Taz2 and 4CA-Taz2. (A) Binding of fluorescein-p53(14−28) to wt Taz2 (filled squares) and MDM2(17−125) (open triangles) as measured by direct fluorescence anisotropy. (B) Binding of p53(14−28) and p53(1−39) to wt Taz2 and 4CA-Taz2 as measured by competition fluorescence anisotropy. wt Taz2 + p53(1−39), filled squares; wt Taz2 + p53(14−28), filled diamonds; 4CA-Taz2 + p53(1−39), open circles. (C) Summary of affinity constants for binding of p53 TAD1 peptides to wt Taz2 (filled squares) and 4CA-Taz2 (open circles).

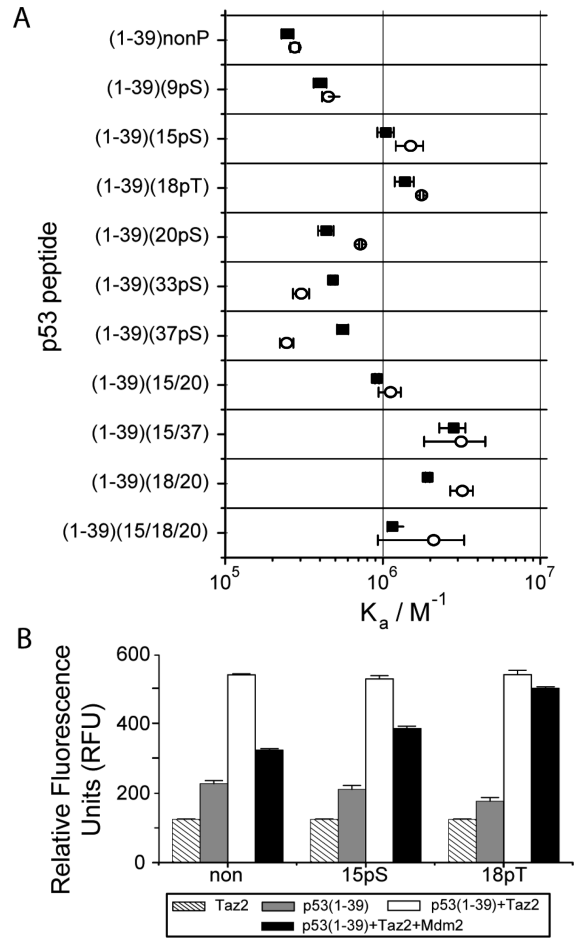

FIGURE 3: Effects of phosphorylation on the binding of p53(1−39) peptides to Taz2 domain proteins. (A) Affinity constants for the binding of phosphorylated p53(1−39) to wt Taz2 (filled squares) and 4CA-Taz2 (open circles) were determined by competitive fluorescence anisotropy. (B) Competition of MDM2(17−125) and 4CA-Taz2 for binding to phosphorylated p53(1−39) was assayed by FRET at 37 °C. Labeled 4CA-Taz2 alone, diagonal bars; fluorescein-p53(1−39) alone, gray bars; fluorescein-p53(1−39) + labeled 4CA-Taz2, white bars; fluorescein-p53(1−39) + labeled 4CA-Taz2 + MDM2(17−125), black bars.

determined association constants for the binding of unlabeled p53 peptides by competition with fluorescein-p53(14−28). The association constant for nonlabeled p53(14−28) ($K_a = 1.3 \times 10^4$ M^{-1}) is about 10-fold lower than the binding of the fluorescein-labeled peptide. Interestingly, p53(1−39), encompassing the entire TAD1, bound to wt Taz2 with 10-fold greater affinity ($K_a = 2.4 \times 10^5$ M^{-1}) (Figure 2B). p53(1−39) also bound to 4CA-Taz2 with a similar affinity as wt Taz2 ($K_a = 2.6 \times 10^5$ M^{-1}). We next synthesized a series of p53 peptides of varying lengths and determined the strength of their binding to Taz2 by competition (Figure 2C). p53(1−39) had the highest affinity for either wt Taz2 or 4CA-Taz2 (Figure 2C). Removal of the N-terminal 4 or 8 amino acids resulted in a 2−5-fold lower affinity. Likewise, removal of 10 residues from the C terminus resulted in 10-fold lower affinity (Figure 2C). Finally, no binding was observed between wt Taz2 and a p53(1−39) mutant in which Leu_{22} and Trp_{23} were mutated to alanine (data not shown), consistent with previous studies showing that these residues are required for the interaction of p53 with p300 (*18, 36*). Thus, the region of p53 that binds to Taz2 is more extensive but includes the region required for MDM2 binding.

Specific Phosphorylations of p53(1−39) Enhance Its Interaction with Taz2. We next examined the effect of specific phosphorylations within p53(1−39) on the binding to Taz2. p53(1−39) peptides were synthesized with mono-, di-, or triphosphorylations corresponding to known sites of modification. We determined the binding of these modified peptides to wt Taz2 or 4CA-Taz2 by the competition fluorescence anisotropy assay (Figure 3A). Phosphorylation of Ser_9 or Ser_{20} resulted in a small increase in the affinity of p53(1−39) for both wt Taz2 and 4CA Taz2. Phosphorylation of Ser_{15} or Thr_{18} produced the greatest effect on binding, increasing the binding affinity by 4-fold and 5-fold, respectively, corresponding to stabilization of complex formation by approximately 0.9 kcal/mol at 25 °C. Phosphorylation of either Ser_{33} or Ser_{37} slightly increased the binding to wt Taz2 but did not affect the affinity for 4CA-Taz2. Thus, phosphorylation of specific amino acids within p53(1−39) increased its binding to Taz2, with modification at Ser_{15} or Thr_{18} having the greatest effect.

The binding affinities of p53(1−39) doubly phosphorylated at Ser_{15} and Ser_{20} for wt Taz2 and 4CA-Taz2 were similar to those of p53(1−39)15pS (Figure 3A). However, the

affinity of wt Taz2 to p53(1−39) diphosphorylated at Thr_{18} and Ser_{20} was significantly higher than the affinity of either respective monophosphorylated peptide. The binding of this peptide to 4CA-Taz2 was slightly higher (Figure 3A). Similarly, p53(1−39) doubly phosphorylated at Ser_{15} and Ser_{37} bound both wt Taz2 or 4CA-Taz2 with higher affinities than either of the monophosphorylated forms (Figure 3A). A fourth diphosphorylated peptide, modified at Ser_{15} and Thr_{18}, was also tested; however, the binding curve for this peptide indicated the presence of an artifactual interaction such that it was not possible to determine the affinity of this peptide for either wt Taz2 or 4CA-Taz2 (data not shown). Triphosphorylation of p53(1−39) at Ser_{15}, Thr_{18}, and Ser_{20} resulted in binding to both wt Taz2 and 4CA-Taz2 with a similar affinity as the diphosphopeptides (Figure 3A). Thus, selected di- or triphosphorylations increased the affinity of p53(1−39) for Taz2 over the monophosphorylated forms. Diphosphorylation of Ser_{15} and Ser_{37} or Thr_{18} and Ser_{20} resulted in the largest increases in binding affinity.

Although both MDM2 and Taz2 bind the TAD1 of p53, the interactions differ in the strength of the binding, the effects of phosphorylations, and the extent of p53 TAD1 involved in binding (see above and ref *37*). In particular, phosphorylation of Thr_{18} has been shown to dramatically decrease the binding of p53 to MDM2 (*19, 27, 37*). Thus we expect TAD1 phosphorylations to affect the ability of Taz2 to compete with MDM2 for binding to p53(1−39) peptides. To provide a qualitative demonstration of this effect, we employed a fluorescence resonance energy transfer (FRET) assay. In the assay, the binding of labeled 4CA-Taz2 to fluorescein-labeled p53(1−39) results in increased fluorescence from the DyLight 549-labeled 4CA-Taz2 when the fluorescein on p53(1−39) is excited. When fluorescently labeled 4CA-Taz2 was incubated with fluorescein-labeled p53(1−39), the fluorescence intensity was greater than the sum of the fluorescence intensities of the labeled 4CA-Taz2 and p53(1−39) samples (Figure 3B). The increased fluorescence suggests the binding of 4CA-Taz2 to p53. When equimolar MDM2(17−125) was added, however, the fluorescence intensity decreased to a level similar to that of the 4CA-Taz2 or p53(1−39) samples, suggesting that the unlabeled MDM2(17−125) displaced the bound, labeled 4CA-Taz2 from p53(1−39). Thus, MDM2(17−125) can compete with Taz2 for binding to p53(1−39). Similarly, incubation of labeled 4CA-Taz2 with fluorescein-labeled p53(1−39)15pS increased fluorescence intensity above the sum of the two separate protein samples (Figure 3B). Addition of MDM2(17−125) decreased the fluorescence intensity to an intermediate level, suggesting that competition for binding to p53(1−39) by MDM2(17−125) is reduced by phosphorylation of Ser_{15}. Finally, when labeled 4CA-Taz2 was incubated with fluorescein-labeled p53(1−39)18pT, the observed fluorescence intensity was not reduced by the addition of MDM2(17−125) (Figure 3B). This result suggests that 4CA-Taz2 bound to p53(1−39)18pT cannot be displaced by MDM2(17−125), consistent with the increased affinity of Taz2 for p53(1−39)18pT and the reduced affinity of MDM2 for this peptide (*27, 37*). Thus, MDM2 is able to compete with Taz2 for binding to p53(1−39), but the competition is affected by the phosphorylation state of p53.

Characterization of the Binding of p53(1−57) to Taz2. While the experiments described above were being performed, a report was published describing the binding of the N terminus of p53 to several domains of p300 and reporting that p53(1−57) showed significantly tighter binding to Taz2 than did p53(1−29) (*30*). To compare the binding of p53(1−57) to that of p53(1−39), we used competition fluorescence anisotropy experiments to measure the binding of 4CA-Taz2 to p53(1−57) and selected phosphorylated derivatives (Table 1). The K_a of p53(1−57) for 4CA-Taz2 was 2×10^6 M^{-1} (Table 1), approximately 8-fold higher than that of p53(1−39). This increased binding affinity of p53(1−57) shows that there are residues between 40−57 that increase the binding between p53 and Taz2. p53(1−57)15pS binds 4CA-Taz2 with an affinity 2-fold higher than that of the nonphosphorylated form (Table 1); similarly, increased binding also was observed for p53(1−57)15pS,20pS and p53(1−57)15pS,18pT,20pS. The increased affinity that results from phosphorylation of Ser_{15} in p53(1−57) corresponds to stabilization of the complex by about 0.4 kcal/mol, considerably less than the stabilization resulting from phosphorylation of Ser_{15} in p53(1−39).

Table 1: Association Constants of 4CA-Taz2 Domain−p53(1−57) Complexes[a]

peptide	$K_a/10^6$ (M^{-1})
p53(1−57)nonP	2.0 ± 0.4
p53(1−57)15pS	4.3 ± 1.8
p53(1−57)15pS,20pS	4.5 ± 1.5
p53(1−57)15pS,18pT,20pS	3.6 ± 1.3

[a] Equilibrium association constants were determined at 25 °C by a fluorescence anisotropy competition assay using fluorescein-labeled p53(14−28).

We next used ITC to gain further insight into the binding of p53(1−57) to Taz2. Initially, experiments were performed in which p53(1−57) was titrated into 4CA-Taz2 at 25 °C. Interestingly, the observed envelope of injection heats differs from the monotonic return to baseline that results from the formation of a 1:1 complex (Figure 4A). Specifically, the integrated injection heats increased up to a molar ratio of approximately 1:1 and then decreased at higher molar ratios, returning to the baseline by a molar ratio of about three p53 peptides per Taz2 protein. Furthermore, in ITC experiments, the presence of two or more binding sites on the macromolecule in the cell does not produce a biphasic envelope of injection heats. Rather, this shape indicates the presence of multiple binding sites on the titrated molecule, p53(1−57), for the molecule in the cell, 4CA-Taz2. To test whether the second binding site may reflect nonspecific electrostatic interactions between the acidic p53(1−57) and the basic Taz2, we repeated the titration with a higher concentration of salt in the buffer. Although the magnitude of the enthalpy change was greatly reduced in the higher salt buffer, the curve shape remained the same (data not shown). Thus, the observed two-site binding was not a nonspecific effect but instead suggested the presence of two Taz2 binding sites in p53(1−57). To provide further evidence for the presence of two binding sites for Taz2 on p53(1−57), we performed ITC titrations in which Taz2 was titrated into p53(1−57) at 25 °C. This reverse titration produced a qualitatively different envelope of injection heats (Figure 4B). Titrations in both formats were fit by a model, described further below, in which Taz2 binds anticooperatively to two sites on p53(1−57).

Taz2 Binds to p53(25−65) with a Similar Affinity as to p53(1−39), but Binding Is Not Affected by Phosphorylation.

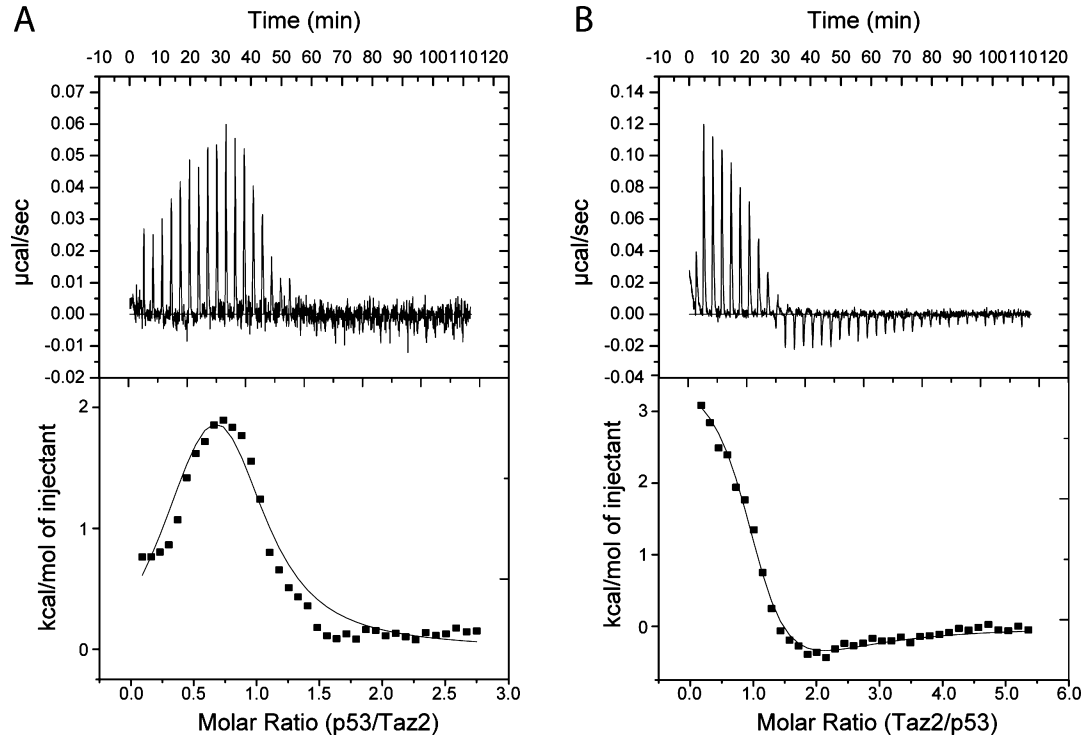

FIGURE 4: ITC characterization of the interaction of p53(1−57) with 4CA-Taz2. (A) Titration of p53(1−57) into 4CA-Taz2 at 25 °C. (B) Titration of 4CA-Taz2 into p53(1−57) at 25 °C. In each panel, the raw data are displayed in the upper figure, and the normalized, integrated injection heats are displayed in the lower panel. The solid lines in the lower figures of both panels reflect the best fit of a model in which Taz2 binds anticooperatively to two sites on p53(1−57).

Table 2: Association Constants of 4CA-Taz2 Domain−p53(25−65) Complexes[a]

peptide	$K_a/10^5$ (M^{-1})
p53(25−65)nonP	3.81 ± 0.19
p53(25−65)46pS	4.33 ± 0.20
p53(25−65)55pT	2.67 ± 0.69
p53(25−65)53A,54A	<0.05

[a] Equilibrium association constants were determined at 25 °C by a fluorescence anisotropy competition assay using fluorescein-labeled p53(14−28).

The transactivation domain of p53 can be divided into two subdomains, the first from residues 1−40 and the second from residues 41−61 (*17, 18*). ITC experiments indicated the presence of two binding sites for Taz2 within p53(1−57), suggesting that Taz2 interacts with both TAD1 and TAD2. We measured the binding of p53(25−65), representing TAD2, to 4CA-Taz2 by competition fluorescence anisotropy and observed that p53(25−65) bound 4CA-Taz2 with a K_a of 3.81 × 10^5 M^{-1} (Table 2), very similar to that for p53(1−39). The observed binding is specific to this site, as a mutant in which Trp_{53} and Phe_{54} were both mutated to alanine showed no observable binding to 4CA-Taz2 (Table 2). This reduction in the interaction is consistent with previous reports that these residues are required for p53 transactivation activity in TAD2 (*17*). Thus, both TAD1 and TAD2 bind to Taz2 with similar affinities.

There are two known sites of posttranslational modification within p53(25−65): phosphorylation at Ser_{46} and at Thr_{55}. To determine if either modification has an effect on Taz2 binding, the modified peptides were assayed for binding by competition fluorescence anisotropy. p53(25−65)46pS and p53(25−65)55pT were found to have similar affinity for 4CA-Taz2 as p53(25−65) (Table 2). Phosphorylation in TAD2, therefore, does not affect binding of this domain of p53 to Taz2.

Taz2 Complexes with TAD1 and TAD2 Have Different Thermodynamic Properties. ITC was next used to better understand the binding of Taz2 to TAD1 and TAD2. Two peptides were used to represent the subdomains: p53(1−39) for TAD1 and p53(35−59) for TAD2. Titrations were performed at 35 °C because the enthalpy for 4CA-Taz2 binding to p53(1−39) is close to zero at 25 °C (see below). The titration of p53(1−39) into 4CA-Taz2 at 35 °C was fit by a 1:1 binding model (Figure 5A). The binding is exothermic, with $\Delta H = -3.5 \pm 0.4$ kcal/mol, and is characterized by the association constant $K_a = 3.74 \times 10^5$ M^{-1}, which is similar to that measured by fluorescence anisotropy at 25 °C. Similarly, p53(35−59) was titrated into 4CA-Taz2 at 35 °C. These titrations were also fit by a one-site binding model (Figure 5B). The binding of p53(35−59) to 4CA-Taz2 is exothermic, with $\Delta H = -3.7 \pm 0.4$ kcal/mol, which is very similar to the enthalpy for 4CA-Taz2 binding to p53(1−39). The association constant for the binding of 4CA-Taz2 to p53(35−59), $K_a = 9.60 \times 10^5$ M^{-1}, is approximately three times larger than that for the binding to p53(1−39).

To develop a more complete understanding of the differences in the binding of 4CA-Taz2 to the two subdomains, titrations were performed at 15, 25, and 35 °C. Each of the two p53 peptides was titrated into 4CA-Taz2, and the resulting normalized, integrated heats of injection were fit to a 1:1 binding model. The changes in enthalpy, entropy, and free energy for the two complexes are shown in Figure 6. The binding of p53(1−39) to 4CA-Taz2 is endothermic at 15 °C and exothermic at 35 °C. The binding of p53(35−59) to 4CA-Taz2 is exothermic at both 25 and 35 °C, but the

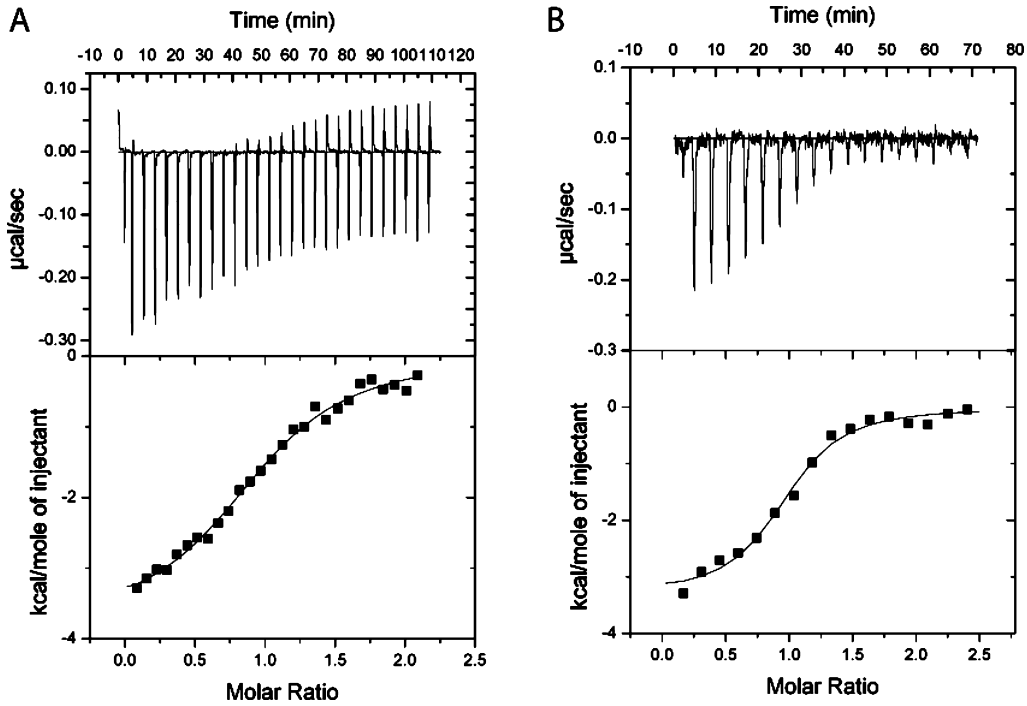

FIGURE 5: ITC curves of the interaction of p53(1−39) (A) and p53(35−59) (B) with 4CA-Taz2. Data are shown for a representative experiment in which p53 was titrated into 4CA-Taz2 at 35 °C. In each panel, the top figure represents the raw data, and the lower figure represents the normalized, integrated injection heats for each point. The solid curves are derived from a 1:1 binding model.

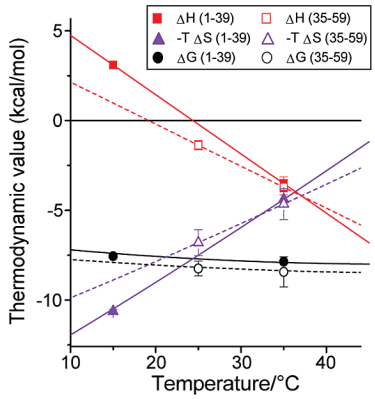

FIGURE 6: Thermodynamic constants for the binding of p53(1−39) or p53(35−59) to 4CA-Taz2, as determined by ITC at 15, 25, and 35 °C. Closed symbols, p53(1−39); open symbols, p53(35−59). Squares, ΔH; triangles, $-T\Delta S$; circles, ΔG. Curves represent the values of the thermodynamic constants predicted by the Gibbs−Helmholtz equation with $\Delta C_p = -330$ cal/(mol·K) (solid curves, p53(1−39)) or $\Delta C_p = -234$ cal/(mol·K) (dotted curves, p53(35−59)).

magnitude is larger at 35 °C. The change upon complex formation in the heat capacity at constant pressure, ΔC_p, can be calculated from the temperature dependence of ΔH. For the interaction between 4CA-Taz2 and p53(1−39), $\Delta C_p = -330$ cal/(mol·K), whereas for the interaction of 4CA-Taz2 and p53(35−59), $\Delta C_p = -234$ cal/(mol·K). A negative ΔC_p suggests that the binding is dominated by hydrophobic interactions (*38, 39*). This conclusion is supported by the loss of binding of p53(1−39) to Taz2 when Leu_{22} and Trp_{23} were mutated to alanines and, similarly, the loss of binding of p53(25−65) when Trp_{53} and Phe_{54} were mutated to alanines. The magnitude of ΔC_p, however, is smaller for 4CA-Taz2 binding to p53(35−59) than to p53(1−39), suggesting differences in the proportion of hydrophobic and electrostatic interactions contributing to the binding at each site (*39, 40*). Due to fundamental thermodynamic linkages, the changes in entropy upon complex formation are also temperature dependent, with the entropic contribution to the free energy of complex formation decreasing with increasing temperature. The large, positive enthalpy of complex formation observed for 4CA-Taz2 binding to p53(1−57) at 25 °C (Figure 4) differed significantly from the enthalpies for 4CA-Taz2 binding to p53(1−39) and to p53(35−59). At 25 °C, the enthalpy for 4CA-Taz2 binding to the isolated TAD1 or TAD2 peptides was near zero or small and negative, respectively. Attempts to fit the ITC titrations of 4CA-Taz2 and p53(1−57) with a model in which the two sites were independent were not successful. However, we were able to fit the calorimetric titrations, both when p53 was titrated into 4CA-Taz2 and when 4CA-Taz2 was titrated into p53(1−57), with a model in which binding to the two sites was anticooperative. The parameters that resulted in the best fit of the data are given in Table 3. The association constant for binding to the stronger site, $K_1 = 3.5 \times 10^6$ M^{-1}, is similar to that observed by the competitive fluorescence anisotropy assay. Binding to the second site is approximately 6 times weaker. The parameter $\alpha = 0.43$ indicates that the

Table 3: Parameters for Two Interacting Site Models of p53(1−57) Binding to 4CA-Taz2[a]

parameter	value
K_1	$3.5 \times 10^6 \pm 4 \times 10^5$ M^{-1}
K_2	$5.2 \times 10^5 \pm 1 \times 10^5$ M^{-1}
α	0.43 ± 0.05
ΔH_1	3300 ± 740 cal/mol
ΔH_2	-1300 ± 370 cal/mol
ΔH_α	-1520 ± 350 cal/mol

[a] K_1 and K_2 are the association constants for binding of 4CA-Taz2 to the first and second sites of p53(1−57), respectively; α is the cooperativity of the interaction between the two sites; ΔH_1 and ΔH_2 are the changes in enthalpy for complex formation at the first and second sites, respectively; ΔH_α is the enthalpy of cooperativity.

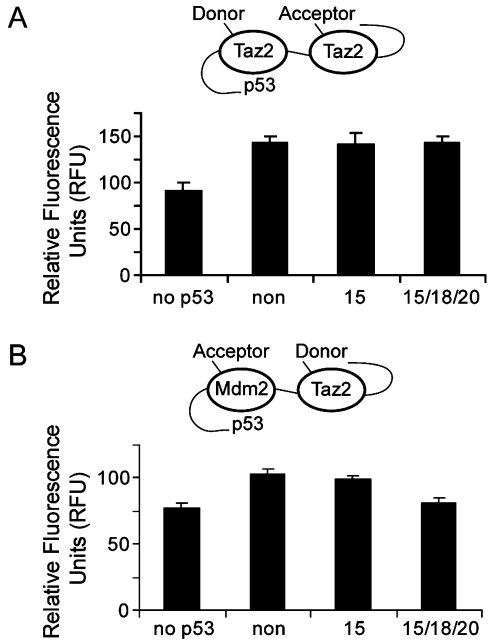

FIGURE 7: Ternary complex formation between p53(1−57) and 4CA-Taz2 and MDM2(17−125). (A) FRET from donor-labeled 4CA-Taz2 to acceptor-labeled 4CA-Taz2 when incubated with p53(1−57) or related phosphorylated peptides. (B) FRET from donor-labeled 4CA-Taz2 to acceptor-labeled MDM2(17−125) when incubated with p53(1−57) or related phosphorylated peptides.

binding of two 4CA-Taz2 molecules to the same p53(1−57) molecule is anticooperative. Possible mechanisms leading to this anticooperativity include repulsion between the bound Taz2 molecules and competition between bound Taz2 molecules for the linker between the two binding sites.

Taz2 and MDM2(17−125) Can Form a Ternary Complex on p53(1−57) That Is Affected by p53 Phosphorylation. To provide additional, qualitative evidence for the binding of two Taz2 molecules to p53(1−57), FRET assays were performed using unlabeled p53(1−57) and two preparations of 4CA-Taz2 that had been separately labeled with fluorescent donor or acceptor moieties. In the absence of p53(1−57), incubation of donor- and acceptor-labeled 4CA-Taz2 produced a low level of fluorescence (Figure 7A). Addition of p53(1−57) increased the fluorescence intensity, suggesting the formation of a ternary complex of two molecules of 4CA-Taz2 bound to p53(1−57). Addition of p53(1−57)15pS or p53(1−57)15pS,18pT,20pS to donor- and acceptor-labeled 4CA-Taz2 increased the fluorescence intensity to a similar degree (Figure 7A). Thus, the FRET assay demonstrates the simultaneous binding of two molecules of Taz2 on p53(1−57), consistent with the ITC experiments.

As Taz2 can bind to both TAD1 and TAD2, we next used the FRET assay to determine qualitatively if Taz2 and MDM2 could simultaneously bind to p53(1−57). In the absence of p53(1−57), incubation of DyLight 488-labeled 4CA-Taz2 with DyLight 549-labeled MDM2(17−125) produced a low level of fluorescence (Figure 7B). Addition of p53(1−57) increased the fluorescence intensity, suggesting the formation of a ternary complex involving p53(1−57), 4CA-Taz2, and MDM2(17−125). A similar level of fluorescence was observed upon addition of p53(1−57)15pS, while fluorescence was reduced to background levels upon addition of p53(1−57)15pS,18pT,20pS. The loss of FRET in the presence of p53(1−57)15pS,18pT,20pS is consistent with the greatly reduced binding of MDM2(17−125) to p53 phosphorylated at those residues (*27, 37*). Thus, MDM2(17−125) is able to form a ternary complex with Taz2 and p53(1−57) that is modulated by p53 phosphorylation.

DISCUSSION

The role of posttranslational modifications in the interactions of p53 with its cofactors is critically important. Here, we have examined the binding of p53 to the Taz2 domain of p300, an acetyltransferase that is known to be a cofactor of several transcription factors. We identified two sites within the first 60 amino acids of p53 that interact with Taz2. The first, p53(1−39), is located in the N-terminal transactivation domain, TAD1. We found that binding of Taz2 in this site is modulated by phosphorylation, with single modifications at Ser_{15} and Thr_{18} increasing binding to Taz2 4−5-fold (Figure 3). Furthermore, diphosphorylation at Ser_{15} and Ser_{37} or Thr_{18} and Ser_{20} increased binding over the respective singly modified forms. However, the triphosphorylated peptide, p53(1−39)15pS,18pT,20pS did not exhibit any further increase in affinity for Taz2 compared with the diphosphorylated form. Thus, phosphorylation within TAD1 modulates the affinity of p53 for one of its coactivators. The second Taz2 binding site, located within residues 35−59 of TAD2, binds with a similar affinity as the first. We found that phosphorylation of either Ser_{46} or Thr_{55} did not affect binding to Taz2.

The N-terminal binding site on p53 has previously been shown to also interact with other proteins, including MDM2. The minimal MDM2 binding domain is defined as p53(14−28), a fragment smaller than is required for binding to Taz2. MDM2 binds p53 tightly, $K_d = 0.6\ \mu M$, to target it for degradation; p53 phosphorylation at Thr_{18} abrogates MDM2 binding (*19, 27*). By comparison, Taz2 binding to unmodified p53 is weaker, but phosphorylation of p53 at Ser_{15} and Thr_{18} increases the affinity of Taz2 for p53 to a level similar to that of MDM2. Thus, phosphorylations in TAD1 have opposite effects on the Taz2 and MDM2 binding: increasing binding for the former and decreasing binding for the latter. Indeed, we found that MDM2(17−125) displaced Taz2 in binding to unphosphorylated p53. Phosphorylation at Ser_{15} moderately reduced the ability of MDM2(17−125) to compete, whereas phosphorylation at Thr_{18} severely reduced the competition for p53 by MDM2(17−125) (Figure 3B). These results are consistent with an earlier report that MDM2 inhibited CBP-mediated p53 transactivation in a model system (*16*) and a recent study showing that inhibition of the MDM2-p53 interaction with the MDM2 inhibitor nutlin-3a increased p53 acetylation and expression of p53 target genes (*41*). Our studies, therefore, provide another example of the importance of p53 posttranslational modifications in the regulation of p53 and its protein−protein interactions. In this case, phosphorylations of p53 in TAD1 shift the equilibrium away from MDM2 binding, with the consequential degradation of p53, and toward Taz2 binding, resulting in target gene transactivation.

Our investigation into the binding of p53 with Taz2 revealed the presence of two binding sites within the N terminus of p53. The possible existence of a second hydrophobic binding site within the first 60 amino acids of p53 has been suggested previously based on the transient

formation of amphipathic β-turns involving residues 40−44 and 48−53 (*42, 43*). MDM2 has also been suggested to be able to bind p53 in both TAD1 and TAD2, although binding to the second domain was estimated to be 20 times weaker than binding to the first (*44*). Ile_{50}, Trp_{53}, and Phe_{54} formed important hydrophobic interactions in binding to MDM2, and it is possible that they do the same for binding to Taz2. Indeed, we found that mutation of Trp_{53} and Phe_{54} to alanine made an interaction between p53(25−65) and Taz2 undetectable.

We further observed that MDM2(17−125) and Taz2 can simultaneously bind to p53(1−57), forming a ternary complex of the three domains (Figure 7B). Previous studies have provided conflicting evidence on the formation of a ternary complex among MDM2, p53, and CBP/p300. Grossman et al. found that a central domain of MDM2 is able to bind CBP through the N-terminal Taz1 domain using residues distinct from those involved in p53 binding and proposed that a ternary complex may be formed in which the N terminus of MDM2 binds to p53 TAD1 while the central portion of MDM2 binds to the Taz1 domain of CBP/p300, which is also bound to the p53 DNA binding domain (*12*). However, a later study suggested that this reported complex may be an experimental artifact (*45*). More recently, the association of p53 and MDM2 in chromatin was found to correlate with repression of transcription, whereas the absence of association of p53 and MDM2 in chromatin correlated with activation of transcription (*46*), suggesting that functional associations of MDM2 and p300 with p53 are mutually exclusive. Our results demonstrate the formation of a ternary complex among the isolated domains *in vitro* but do not address the behavior of the intact proteins in a physiological setting.

The presence of the second binding site explains the observed increase in binding of p53(1−57) to Taz2 compared with p53(1−39); the former fragment contains both Taz2 binding sites, leading to increased overall binding as observed by competition fluorescence anisotropy. A recent study of p300−p53 binding reported a significantly tighter interaction between p53(1−57) and Taz2 than we observed (*30*). The difference in binding constants likely results from technical differences in the binding assays. Using NMR titration experiments, the authors further determined that p53 interacts with Taz2 through an extended interface, as amide resonances were found to disappear for most p53 residues from 10−56 upon binding to Taz2 (*30*). These NMR results are also consistent with the presence of two Taz2 binding sites on p53, as directly shown by the experiments presented here. Though the binding of Taz2 to the two sites in p53(1−57) is anticooperative, both affinities are indicative of relatively tight binding (Table 3). At the high sample concentrations used in NMR spectroscopy, p53 molecules with one Taz2 bound to TAD1, with one Taz2 bound to TAD2, and with two Taz2 molecules bound would exist in equilibrium, suggesting an explanation for the large number of p53 amide resonances that disappeared in the NMR spectra.

Alignment of the residues of p53(1−39) and p53(40−64) highlights the sequence similarity in the two binding sites (Figure 8). Both domains contain a Φ-X-X-Φ-Φ motif (where Φ is a hydrophobic amino acid) that has been shown to be important for many protein−protein interactions. When the final two hydrophobic residues in either binding site,

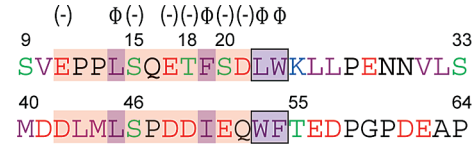

FIGURE 8: Alignment of the TAD1 and TAD2 primary sequences. Amino acids are colored according to their side chains, with hydrophobic residues shown in purple text, polar uncharged residues in green text, acidic residues in red text, and basic residues in blue text. Those amino acids that make up the Φ-X-X-Φ-Φ motif are highlighted in purple, and the residues that align best between the two domains are highlighted in tan. The hydrophobic residues that are known to be required for binding and p53 transactivation, Leu_{22}/Trp_{23} and Trp_{53}/Phe_{54}, are boxed.

Leu_{22} and Trp_{23} in TAD1 or Trp_{53} and Phe_{54} in TAD2, were mutated to alanine, we were unable to observe binding between p53 and Taz2. In TAD2, the first hydrophobic residue in the motif, Ile_{50}, is surrounded by acidic residues; a similar charge state is obtained in TAD1 upon phosphorylation of Thr_{18} and Ser_{20}, two modifications that increase the affinity of p53 (1−39) for Taz2 (Figure 3A). It is possible that the difference in ΔC_p for the binding of 4CA-Taz2 to p53(1−39) and p53(35−59) reflects this difference in the number and location of acidic residues in the nonphosphorylated forms. Since electrostatic and hydrophobic interactions are thought to contribute with opposite signs to the value of ΔC_p (*40*), the less negative value of ΔC_p for p53(35−59) may be due to the greater number of acidic residues in TAD2 that interact electrostatically with the basic Taz2. The alignment of the two binding sites also suggests an explanation for the lack of effect of Thr_{55} phosphorylation on the binding of p53(25−65) to TAZ2. In TAD1, the corresponding residue is Lys_{24}, indicating that a charge at this site is not important for binding to Taz2. However, it is interesting to note that although Ser_{46} aligns with Ser_{15}, phosphorylation of Ser_{46} does not affect binding whereas modification of Ser_{15} increases binding. A possible explanation for this discrepancy is that the linear alignment shown in Figure 8 incompletely represents the structural features of the two domains. The different values of ΔC_p characterizing the binding of the TAD1 and TAD2 peptides to 4CA-Taz2 suggest differences in the binding of the two domains to Taz2, and thus structural differences between the two complexes may account for the observed differences in the effects of phosphorylation. Furthermore, the phosphorylations of Ser_{15} and Ser_{46} are effected by different kinases (*26*), suggesting that the two sites are both distinctly regulated and have distinct roles in the response to stress. For example, UV damage has been found to induce phosphorylation of Ser_{46} but not Ser_{15} (*47*). Also, as TAD2 has been shown to be important in recruiting the STAGA transcriptional coactivator complex (*48*), phosphorylation of Ser_{46} may play a distinct role from phosphorylation of Ser_{15} in coactivator recruitment following stress. We are currently pursuing structural studies of the complex of Taz2 and p53 that may provide additional details concerning which residues are important for binding.

In our *in vitro* binding assays, the modeling of the ITC data suggested anticooperativity in the binding of two Taz2 molecules to p53(1−57) (Table 3). It is possible that this observed anticooperativity is due to steric hindrance in binding two Taz2 molecules. Alternatively, the linker region between the two TADs could play a role in binding, and

thus, binding of the second molecule of Taz2 is weaker because the linker is already bound. It seems unlikely, however, that two p300 molecules would simultaneously bind a single p53 N terminus in the cell due to the limiting amounts of p300 and its many interactors.

The identification of a second Taz2 binding region within a short distance of the first raises the question of why there are multiple binding sites for a single domain of a protein. Furthermore, the N terminus of p53 has been shown to interact with five different domains of p300, including Taz2, most of which show some increased affinity upon p53 modification (*10, 30, 31, 49*). It is possible, then, that p53 acts as a many-to-one logical control element. Within these two transactivation domains are phosphorylation sites for many different kinases involved in various signaling pathways (*26*). Thus, modifications on p53 that modulate its protein−protein interactions may act to integrate these disparate signaling pathways into a single response. Genotoxic stresses that activate these signaling cascades require quick cellular responses, including cell cycle arrest or apoptosis (*50*).

It is also possible that the high local concentration of binding sites increases the net association of p300 and p53. As a transcriptional coactivator, p300 interacts with a number of other proteins and is part of the transcription machinery. Likewise, the N terminus of p53 is known to bind many proteins, indicating a competition for binding to the specific partner for the required response. Having multiple binding sites increases the chances of binding; furthermore, the combination of several lower affinity binding sites results in one high-affinity interaction. One study found the affinity of the N terminus of p53 for the full p300 protein to be 10−100-fold tighter than the affinity for some of its domains, and phosphorylation of this domain of p53 increases that affinity 4−10-fold (*31*). Therefore, combining multiple binding sites for the same protein may allow the p53−p300 complex to form in the presence of many other potential binding partners, with the affinities of these multiple interactions modulated by p53 phosphorylation. In a model cellular system designed to study chromatin structure, Carpenter et al. found that the number of acidic activation motifs correlated with increased extent of chromatin unwinding (*51*). The observed chromatin unwinding was a common property of acidic activation domains, including the TAD of p53.

In the present study, we have investigated the effect of p53 phosphorylation on its interaction with Taz2. We found that phosphorylation can increase the binding of p53(1−39) to Taz2, with phsophorylation at Ser_{15} and Thr_{18} having the greatest effect on binding. We further defined a second Taz2 binding site of comparable affinity within TAD2; phosphorylation of p53 within this second site did not affect binding. Thus, we have demonstrated that p53 interacts with Taz2 through two sites. Furthermore, we have provided another example of the importance of p53 posttranslational modification in the regulation of its activity, specifically by increasing its binding to a crucial transcriptional coactivator.

ACKNOWLEDGMENT

We thank Thomas Burlin (NIMH, NIH) for amino acid composition analysis.

REFERENCES

1. Das, S., Boswell, S. A., Aaronson, S. A., and Lee, S. W. (2008) P53 promoter selection: choosing between life and death. *Cell Cycle 7*, 154–157.
2. Barlev, N. A., Liu, L., Chehab, N. H., Mansfield, K., Harris, K. G., Halazonetis, T. D., and Berger, S. L. (2001) Acetylation of p53 activates transcription through recruitment of coactivators/histone acetyltransferases. *Mol. Cell 8*, 1243–1254.
3. Liu, G., Xia, T., and Chen, X. (2003) The activation domains, the proline-rich domain, and the C-terminal basic domain in p53 are necessary for acetylation of histones on the proximal p21 promoter and interaction with p300/CREB-binding protein. *J. Biol. Chem. 278*, 17557–17565.
4. Gu, W., and Roeder, R. G. (1997) Activation of p53 sequence-specific DNA binding by acetylation of the p53 C-terminal domain. *Cell 90*, 595–606.
5. Sakaguchi, K., Herrera, J. E., Saito, S., Miki, T., Bustin, M., Vassilev, A., Anderson, C. W., and Appella, E. (1998) DNA damage activates p53 through a phosphorylation-acetylation cascade. *Genes Dev. 12*, 2831–2841.
6. Ponting, C. P., Blake, D. J., Davies, K. E., Kendrick-Jones, J., and Winder, S. J. (1996) ZZ and TAZ: new putative zinc fingers in dystrophin and other proteins. *Trends Biochem. Sci. 21*, 11–13.
7. Parker, D., Ferreri, K., Nakajima, T., LaMorte, V. J., Evans, R., Koerber, S. C., Hoeger, C., and Montminy, M. R. (1996) Phosphorylation of CREB at Ser-133 induces complex formation with CREB-binding protein via a direct mechanism. *Mol. Cell. Biol. 16*, 694–703.
8. Goodman, R. H., and Smolik, S. (2000) CBP/p300 in cell growth, transformation, and development. *Genes Dev. 14*, 1553–1577.
9. Lin, C. H., Hare, B. J., Wagner, G., Harrison, S. C., Maniatis, T., and Fraenkel, E. (2001) A small domain of CBP/p300 binds diverse proteins: solution structure and functional studies. *Mol. Cell 8*, 581–590.
10. Dornan, D., Shimizu, H., Perkins, N. D., and Hupp, T. R. (2003) DNA-dependent acetylation of p53 by the transcription coactivator p300. *J. Biol. Chem. 278*, 13431–13441.
11. Avantaggiati, M. L., Ogryzko, V., Gardner, K., Giordano, A., Levine, A. S., and Kelly, K. (1997) Recruitment of p300/CBP in p53-dependent signal pathways. *Cell 89*, 1175–1184.
12. Grossman, S. R., Perez, M., Kung, A. L., Joseph, M., Mansur, C., Xiao, Z. X., Kumar, S., Howley, P. M., and Livingston, D. M. (1998) p300/MDM2 complexes participate in MDM2-mediated p53 degradation. *Mol. Cell 2*, 405–415.
13. Gu, W., Shi, X. L., and Roeder, R. G. (1997) Synergistic activation of transcription by CBP and p53. *Nature 387*, 819–823.
14. Livengood, J. A., Scoggin, K. E., Van Orden, K., McBryant, S. J., Edayathumangalam, R. S., Laybourn, P. J., and Nyborg, J. K. (2002) p53 Transcriptional activity is mediated through the SRC1-interacting domain of CBP/p300. *J. Biol. Chem. 277*, 9054–9061.
15. Van Orden, K., Giebler, H. A., Lemasson, I., Gonzales, M., and Nyborg, J. K. (1999) Binding of p53 to the KIX domain of CREB binding protein. A potential link to human T-cell leukemia virus, type I-associated leukemogenesis. *J. Biol. Chem. 274*, 26321–26328.
16. Wadgaonkar, R., and Collins, T. (1999) Murine double minute (MDM2) blocks p53-coactivator interaction, a new mechanism for inhibition of p53-dependent gene expression. *J. Biol. Chem. 274*, 13760–13767.
17. Candau, R., Scolnick, D. M., Darpino, P., Ying, C. Y., Halazonetis, T. D., and Berger, S. L. (1997) Two tandem and independent sub-activation domains in the amino terminus of p53 require the adaptor complex for activity. *Oncogene 15*, 807–816.
18. Chang, J., Kim, D. H., Lee, S. W., Choi, K. Y., and Sung, Y. C. (1995) Transactivation ability of p53 transcriptional activation domain is directly related to the binding affinity to TATA-binding protein. *J. Biol. Chem. 270*, 25014–25019.
19. Bottger, V., Bottger, A., Garcia-Echeverria, C., Ramos, Y. F., van der Eb, A. J., Jochemsen, A. G., and Lane, D. P. (1999) Comparative study of the p53-mdm2 and p53-MDMX interfaces. *Oncogene 18*, 189–199.
20. Oliner, J. D., Pietenpol, J. A., Thiagalingam, S., Gyuris, J., Kinzler, K. W., and Vogelstein, B. (1993) Oncoprotein MDM2 conceals the activation domain of tumour suppressor p53. *Nature 362*, 857–860.
21. Kussie, P. H., Gorina, S., Marechal, V., Elenbaas, B., Moreau, J., Levine, A. J., and Pavletich, N. P. (1996) Structure of the MDM2

oncoprotein bound to the p53 tumor suppressor transactivation domain. *Science 274*, 948–953.
22. Abramova, N. A., Russell, J., Botchan, M., and Li, R. (1997) Interaction between replication protein A and p53 is disrupted after UV damage in a DNA repair-dependent manner. *Proc. Natl. Acad. Sci. U.S.A. 94*, 7186–7191.
23. Di Lello, P., Jenkins, L. M. M., Jones, T. N., Nguyen, B. D., Hara, T., Yamaguchi, H., Dikeakos, J. D., Appella, E., Legault, P., and Omichinski, J. G. (2006) Structure of the Tfb1/p53 complex: Insights into the interaction between the p62/Tfb1 subunit of TFIIH and the activation domain of p53. *Mol. Cell 22*, 731–740.
24. Leiter, L. M., Chen, J., Marathe, T., Tanaka, M., and Dutta, A. (1996) Loss of transactivation and transrepression function, and not RPA binding, alters growth suppression by p53. *Oncogene 12*, 2661–2668.
25. Xiao, H., Pearson, A., Coulombe, B., Truant, R., Zhang, S., Regier, J. L., Triezenberg, S. J., Reinberg, D., Flores, O., Ingles, C. J., and Greenblatt, J. (1994) Binding of basal transcription factor TFIIH to the acidic activation domains of VP16 and p53. *Mol. Cell Biol. 14*, 7013–7024.
26. Appella, E., and Anderson, C. W. (2001) Post-translational modifications and activation of p53 by genotoxic stresses. *Eur. J. Biochem. 268*, 2764–2772.
27. Craig, A. L., Burch, L., Vojtesek, B., Mikutowska, J., Thompson, A., and Hupp, T. R. (1999) Novel phosphorylation sites of human tumour suppressor protein p53 at Ser20 and Thr18 that disrupt the binding of mdm2 (mouse double minute 2) protein are modified in human cancers. *Biochem. J. 342*, 133–141.
28. Lambert, P. F., Kashanchi, F., Radonovich, M. F., Shiekhattar, R., and Brady, J. N. (1998) Phosphorylation of p53 serine 15 increases interaction with CBP. *J. Biol. Chem. 273*, 33048–33053.
29. Dumaz, N., and Meek, D. W. (1999) Serine15 phosphorylation stimulates p53 transactivation but does not directly influence interaction with HDM2. *EMBO J. 18*, 7002–7010.
30. Teufel, D. P., Freund, S. M., Bycroft, M., and Fersht, A. R. (2007) Four domains of p300 each bind tightly to a sequence spanning both transactivation subdomains of p53. *Proc. Natl. Acad. Sci. U.S.A. 104*, 7009–7014.
31. Polley, S., Guha, S., Kar, S., Roy, N. S., Sakaguchi, K., Chuman, Y., V., S., Kundu, T., and Roy, S. (2008) Differential recognition of phosphorylated transactivation domains of p53 by different p300 domains. *J. Mol. Biol. 376*, 8–12.
32. Hara, T., Durell, S. R., Myers, M. C., and Appella, D. H. (2006) Probing the structural requirements of peptoids that inhibit HDM2-p53 interactions. *J. Am. Chem. Soc. 128*, 1995–2004.
33. Pace, C. N., Vajdos, F., Fee, L., Grimsley, G., and Gray, T. (1995) How to measure and predict the molar absorption coefficient of a protein. *Protein Sci. 4*, 2411–2423.
34. Roehrl, M. H., Wang, J. Y., and Wagner, G. (2004) A general framework for development and data analysis of competitive high-throughput screens for small-molecule inhibitors of protein-protein interactions by fluorescence polarization. *Biochemistry 43*, 16056–16066.
35. De Guzman, R. N., Liu, H. Y., Martinez-Yamout, M., Dyson, H. J., and Wright, P. E. (2000) Solution structure of the TAZ2 (CH3) domain of the transcriptional adaptor protein CBP. *J. Mol. Biol. 303*, 243–253.
36. Lin, J., Chen, J., Elenbaas, B., and Levine, A. J. (1994) Several hydrophobic amino acids in the p53 amino-terminal domain are required for transcriptional activation, binding to mdm-2 and the adenovirus 5 E1B 55-kD protein. *Genes Dev. 8*, 1235–1246.
37. Sakaguchi, K., Saito, S., Higashimoto, Y., Roy, S., Anderson, C. W., and Appella, E. (2000) Damage-mediated phosphorylation of human p53 threonine 18 through a cascade mediated by a casein 1-like kinase. Effect on Mdm2 binding. *J. Biol. Chem. 275*, 9278–9283.
38. Baldwin, R. L. (1986) Temperature dependence of the hydrophobic interaction in protein folding. *Proc. Natl. Acad. Sci. U.S.A. 83*, 8069–8072.
39. Livingstone, J. R., Spolar, R. S., and Record, M. T., Jr. (1991) Contribution to the thermodynamics of protein folding from the reduction in water-accessible nonpolar surface area. *Biochemistry 30*, 4237–4244.
40. Prabhu, N. V., and Sharp, K. A. (2005) Heat capacity in proteins. *Annu. Rev. Phys. Chem. 56*, 521–548.
41. Kumamoto, K., Spillare, E. A., Fujita, K., Horikawa, I., Yamashita, T., Appella, E., Nagashima, M., Takenoshita, S., Yokota, J., and Harris, C. C. (2008) Nutlin-3a activates p53 to both down-regulate inhibitor of growth 2 and up-regulate mir-34a, mir-34b, and mir-34c expression, and induce senescence. *Cancer Res. 68*, 3193–3203.
42. Lee, H., Mok, K. H., Muhandiram, R., Park, K. H., Suk, J. E., Kim, D. H., Chang, J., Sung, Y. C., Choi, K. Y., and Han, K. H. (2000) Local structural elements in the mostly unstructured transcriptional activation domain of human p53. *J. Biol. Chem. 275*, 29426–29432.
43. Vise, P. D., Baral, B., Latos, A. J., and Daughdrill, G. W. (2005) NMR chemical shift and relaxation measurements provide evidence for the coupled folding and binding of the p53 transactivation domain. *Nucleic Acids Res. 33*, 2061–2077.
44. Chi, S. W., Lee, S. H., Kim, D. H., Ahn, M. J., Kim, J. S., Woo, J. Y., Torizawa, T., Kainosho, M., and Han, K. H. (2005) Structural details on mdm2-p53 interaction. *J. Biol. Chem. 280*, 38795–38802.
45. Matt, T., Martinez-Yamout, M. A., Dyson, H. J., and Wright, P. E. (2004) The CBP/p300 TAZ1 domain in its native state is not a binding partner of MDM2. *Biochem. J. 381*, 685–691.
46. White, D. E., Talbott, K. E., Arva, N. C., and Bargonetti, J. (2006) Mouse double minute 2 associates with chromatin in the presence of p53 and is released to facilitate activation of transcription. *Cancer Res. 66*, 3463–3470.
47. Bulavin, D. V., Saito, S., Hollander, M. C., Sakaguchi, K., Anderson, C. W., Appella, E., and Fornace, A. J., Jr. (1999) Phosphorylation of human p53 by p38 kinase coordinates N-terminal phosphorylation and apoptosis in response to UV radiation. *EMBO J. 18*, 6845–6854.
48. Gamper, A. M., and Roeder, R. G. (2008) Multivalent binding of p53 to the STAGA complex mediates coactivator recruitment after UV damage. *Mol. Cell. Biol. 28*, 2517–2527.
49. Finlan, L., and Hupp, T. R. (2004) The N-terminal interferon-binding domain (IBiD) homology domain of p300 binds to peptides with homology to the p53 transactivation domain. *J. Biol. Chem. 279*, 49395–49405.
50. Vousden, K. H. (2006) Outcomes of p53 activation—spoilt for choice. *J. Cell Sci. 119*, 5015–5020.
51. Carpenter, A. E., Memedula, S., Plutz, M. J., and Belmont, A. S. (2005) Common effects of acidic activators on large-scale chromatin structure and transcription. *Mol. Cell. Biol. 25*, 958–968.

BI801716H